Journal of Surface Engineered Materials and Advanced Technology, 2022, 12, 61-81
https://www.scirp.org/journal/jsemat
ISSN Online: 2161-489X
ISSN Print: 2161-4881

Malus domestica and *Solanum lycopersicum* Mixtures for the Synthesis of Graphene Silver and Zinc Oxide Nanocomposites

Rachel Fanelwa Ajayi[1*], Siphokazi Tshoko[1], Candice Franke[1], Nokwanda Ngema[1], Veli Thipe[2], Takalani Mulaudzi[3]

[1]SensorLab, Department of Chemistry, University of the Western Cape, Bellville, South Africa
[2]Laboratório de Ecotoxicologia, Centro de Química e Meio Ambiente, Instituto de Pesquisas Energéticas e Nucleares (IPEN), Comissão Nacional de Energia Nuclear (IPEN/CNEN-SP), São Paulo, Brazil
[3]Department of Biotechnology, University of the Western Cape, Bellville, South Africa
Email: *fngece@uwc.ac.za

How to cite this paper: Ajayi, R.F., Tshoko, S., Franke, C., Ngema, N., Thipe, V. and Mulaudzi, T. (2022) *Malus domestica* and *Solanum lycopersicum* Mixtures for the Synthesis of Graphene Silver and Zinc Oxide Nanocomposites. *Journal of Surface Engineered Materials and Advanced Technology*, **12**, 61-81.
https://doi.org/10.4236/jsemat.2022.124005

Received: October 1, 2022
Accepted: October 28, 2022
Published: October 31, 2022

Abstract

This study reports on the novel and simple green method involving the use of apple (*Malus domestica*) and tomato (*Solanum lycopersicum*) extracts in the synthesis of electroactive layers of silver nanoparticles|graphene oxide (AgNPs|GO) and zinc oxide nanoparticles|graphene oxide (ZnONPs|GO). The surface morphology of the green synthesized nanocomposites was studied using High-Resolution Transmission Electron Microscopy (HRTEM), High-Resolution Scanning Electron Microscopy (HRSEM) while the elemental analysis was studied using Fourier Transform Infrared Spectroscopy (FTIR), Raman spectroscopy and X-Ray diffraction (XRD) and their optical properties were further characterised using Ultraviolet Spectroscopy (UV-vis). The electrochemical studies of these nanocomposites were achieved using cyclic voltammetry (CV) where an increase in electron conductivity of the AgNPs|GO and ZnONPs|GO nanocomposite was observed. Comparatively, the silver nanoparticulate-based platforms were observed to have superior electrochemical properties as opposed to the zinc oxide-based platform. The observed electrochemical activities of the synthesized nanocomposites are a good indication of their suitability as electroactive platforms towards the development of electrochemical sensors. Electrochemical sensors are popular in the Electrochemistry field because they may be developed using different methods in order to suit their intended analytes. As such, the synthesis of a variety of electrochemical platforms provides researchers with a vast range of options to select from for the detection of analytes.

Keywords

Zinc Oxide, Electrochemical Sensors, Silver Nanoparticles, Graphene Oxide, Nanocomposites, *Malus domestica*, *Solanum lycopersicum*, Electrochemistry

1. Introduction

Metal based materials are commonly regarded as nanoparticles (nano silver, nano gold etc.), quantum dots and oxides with metal bases. Nanoparticles of metals and metal oxides are identified to exhibit improved chemical activities and unique reactivities because of the presence of different surface crystal planes, high density of surface atoms and surface relaxations between layers [1] [2] [3] [4]. The primary focus in the last decade has been the development of green chemical methods for the synthesis of metal nanoparticles; hence, a majority of researchers have gained interest in investigating mechanisms of metal ions application and bio-reduction and understanding the possible mechanisms of metal nanoparticle formation. As such, green chemistry has been studied and has found eco-friendly methods for the production of well-characterized nanoparticles. Nanoparticles prepared by green methods have low toxicity and are more stable thus, the preparation of nanoparticles using plant materials provides the most suitable environment [5] [6] [7].

Furthermore, a variety of other green reductants such as microorganisms, glucose, plant extracts, amino acids, vitamin C, ascorbic acid and bovine serum albumin have been found to be useful for synthesizing metallic nanoparticles [8] [9]. A study by Alamdari *et al.* [10] illustrates this possibility through the preparation of zinc oxide nanoparticles using leaf extracts of *Sambucus ebulus*. Similarly, the use of *Prunus amygdalus* was explored for the green synthesis of silver nanoparticles in a study by Srikar *et al.*, 2015 [11]. In contrast, the nanoparticles prepared by chemical methods have been reported to be less suitable for biological activities because of their toxicity and their lack of affordability. Additionally, there is a great interest in incorporating nanoparticles in graphene oxide sheets to form graphene-based nanocomposites. These materials have unique structures and excellent properties that have allowed them to emerge as a class of fascinating materials with promising electrochemical applications. The high surface area of graphene oxide is also essential for dispersing the nanoparticles to sustain their electrochemical activities [12]. Also, nanoparticles supported by graphene oxide maximize the accessibility of the nanosized surface area for electron transfer. They also create enhanced mass transport of the reactants to the electroactive sites on the electrode surfaces. Furthermore, conductive graphene oxide supports also ensure the collection of nanomaterials and the transfer of electrons to the collecting electrode surface. Nonetheless, the functionalization of graphene oxide with nanoparticles has made nanoscale composite electrode modifications promising. Due to that, most recently plant extracts have also

been effectively used to reduce graphene oxide while a sequence of metallic nanoparticles has also been prepared using plant extracts as reducing agents, and their application in the synthesis of graphene-based nanocomposites has so far been admirable [13] [14] [15]. Li *et al.*, 2013 [16] reported the use of green synthesized graphene|silver electroactive sensors for the detection of tryptophan. In a similar study, the one-step green synthesis of graphene|zinc nanocomposites for the nonenzymatic sensing of hydrogen peroxide is also reported [17].

Figure 1 illustrates the novel green method synthesis of silver (Ag) and zinc oxide (ZnO) nanocomposites produced in this study using mixtures of *Solanum lycopersicum* and *Malus domestica*. *Solanum lycopersicum* (tomato) is a member of the Solanaceae family and is known to be a good source of Vitamins C and A. The most abundant organic compounds found in tomatoes are citric acid, ascorbic acid, malic acid, proteins and amino acids thus, it is believed that ascorbic acid and citric acid in the aqueous extract of tomato juice are responsible for reducing metal salts [18] [19] [20]. The success of *Solanum lycopersicum* is illustrated in a study by Sutradhar *et al.*, 2016 [21] reporting on the use of *Solanum lycopersicum* in the synthesis of zinc oxide nanoparticles for photovoltaic application. *Malus domestica* (apples) are acquired from the medium-sized tree belonging to the Rosaceae family. They are rich in phytonutrients, antioxidants, polyphenolics and flavonoids which are believed to play an important role in synthesizing nanoparticles, alongside procyanidin B2, epicatechin, and quercetin [22] [23]. Research work by Ali *et al.*, 2015 [24] and Kazlagić *et al.*, 2020 [25] have reported on the successful use of apple extracts for the synthesis of AgNPs and to also explore their antimicrobial properties. Furthermore, Alves *et al.*, 2019 [26] reported on the use of apple phytochemicals in the synthesis of ZnONPs and their potential biomedical applications. Although there are some reports on the synthesis of AgNPs and ZnONPs from fruits and vegetables, to the best of our knowledge there are no available reports on the mixture of *Malus*

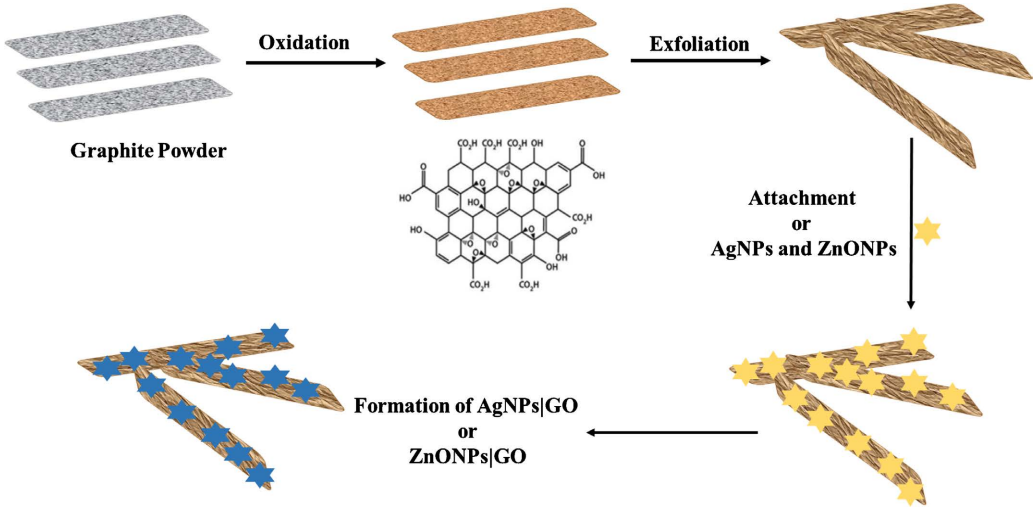

Figure 1. A representation of the green method for the synthesis of AgNPs/GO and ZnONPs/GO nanocomposites using a mixture of *Malus domestica* and *Solanum lycopersicum* extracts.

domestica and *Solanum lycopersicum* extracts for the reduction of metal salts to synthesize nanoparticles coupled to graphene sheets. Thus, we report for the first time an inexpensive one-pot synthesis of AgNPs|GO and ZnONPs|GO nanocomposites through a green methodology stabilised using *Malus domestica* and *Solanum lycopersicum* extracts.

2. Materials and Methods

2.1. Reagents and Materials

All reagents used in this study were of analytical grade and used without any further modification or purification. The reagents include dimethylformamide (DMF), ammonia (NH_3 99.98%), ethanol (CH_3CH_2OH 99.5%), sodium phosphate monobasic dehydrate ($H_2NaPO_4{\cdot}2H_2O$, >99%), disodium hydrogen phosphate dibasic ($Na_2PO_4{\cdot}2H_2O$ > 98%), zinc nitrate ($Zn(NO_3)_2$) and silver nitrate ($AgNO_3$) which were all purchased from Merck, South Africa. Red apples (*Malus domestica*) and tomatoes (*Solanum lycopersicum*) were purchased from Spar supermarket in Belhar, Cape Town, South Africa. Prior to the synthesis of the nanocomposites, all glassware used was cleaned in freshly acidic solutions comprising 1:3 HNO_3/HCl followed by thoroughly rinsing with deionized water and oven drying to ensure thorough cleaning of the glassware. The supporting electrolyte in all the experiments was 0.1 M phosphate buffer solution (PBS), pH 7.4 prepared by mixing stock standard solutions of sodium and dihydrogen phosphate monobasic. Unless otherwise stated, all experiments were conducted at 16˚C - 20˚C. The glassy carbon electrodes used in this study were cleaned by polishing on alumina micro polish obtained from Buehler, IL, USA prior to any modification.

2.2. Instrumentation

Electrochemical responses of the tomato and apple extract (TAE) mediated AgNPs|GO and ZnONPs|GO nanocomposites were investigated using cyclic voltammetry (CV) under aerobic conditions. CV experiments were performed in 0.1 M PBS over a potential window range of +1.0 V to −1.5 V and scanned at various scan rates (10-100 mV/s) for both nanocomposites. The voltammograms were acquired using a PalmSens 3 Potentiostat (PalmSens BV, Houten, The Netherlands) connected to a three-electrode system comprising of a platinum wire counter electrode, a 3.00 mm diameter glassy carbon working electrode and an Ag|AgCl (3 M NaCl type) reference electrode. The characteristic functional groups of TAE|AgNPs|GO and TAE|ZnONPs|GO were measured using Fourier-transformed infrared (FTIR) spectra recorded on a PerkinElmer Spectrum 100-FT-IR Spectrometer (PerkinElmer (Pty) Ltd., Midrand, South Africa) in the region of 400 to 4000 cm^{-1} wavenumbers. Ultraviolet-visible (UV–Vis) absorption measurements for the developed nanocomposites were determined using 1 cm quartz cuvettes in a Nicolet Evolution 100 UV-visible spectrophotometer (Thermo Electron Corporation, Johannesburg, South Africa) over the wavelength range of 200 to 800 nm. The composition and morphological properties

of the nanocomposites were determined using high-resolution transmission electron microscopy (HRTEM) Tecnai G2 F2O X-Twin (FEI Company, Hillsboro, OR, USA), high-resolution scanning electron microscopy (HRSEM, Zeiss Auriga S40) operating at 50 kV (Carl Zeiss Microscopy GmbH, Jena, Germany) and an X-Ray diffraction (XRD) Model Bruker AXS D8 advance with radiation λCukα1 =1.5406 Å (Bruker South Africa Pty Ltd, Sandton, South Africa.

2.3. Preparation of Tomato and Apple Extracts (TAE)

50 g of apple and 50 g of tomato were finely cut and thoroughly washed with distilled water. The skin of both fruits was kept intact before the cutting process. After several attempts, this combination was found to be best suited for the synthesis of nanocomposites. Thereafter, they were combined in a 500 ml conical flask with 200 ml deionized water followed by heating and stirring for 1 hour at 80˚C using an oil bath. The resultant solution in the flask was allowed to reach room temperature and then filtered to obtain the extract.

2.4. Synthesis of |AgNPs|GO Nanocomposite

GO was synthesized from natural graphite powder using the modified Hummers method [27]. AgNPs|GO nanocomposite was prepared by reducing silver ions directly on GO with the apple and tomato extract (TAE) as a reducing and stabilizing agent. 15 mg of GO powder was dispersed in 15 mL of deionized water by ultrasonication for 60 minutes to form a stable GO colloid and then 40 mL of the TAE was dissolved in this solution under stirring. Secondly, 1.1 mL of ammonia was added slowly to 0.2 g of silver nitrate solution until the AgOH|Ag_2O precipitate dissolved. Subsequently, the $Ag(NH_3)_2OH$ solution was mixed with the GO and the extract-containing solution and stirred for 30 minutes. The mixture was then allowed to sit undisturbed at room temperature for 2 hours followed by centrifugation of the slurry-like product which was washed with distilled water repeatedly to remove any impurities. Finally, the obtained product was dried overnight in an oven at 60˚C indicating the formation of the AgNPs|GO nanocomposite. For comparative purposes, AgNPs and ZnONPs were also synthesized using both conventional and microwave-assisted methods to ensure that all the findings indicated in the nanocomposites would be accounted for. The conventional synthesis of AgNPs took place under dark conditions where the conical flask was covered in foil to avoid light that would oxidize the silver ions. The synthesis was prepared by using 40 mL of the prepared extract in 180 mL of 0.1 M aqueous $AgNO_3$ solution. The mixture was stirred and heated at 80˚C for 1 hour and allowed to cool at room temperature prior to storage in a dark bottle. Alternatively, the microwave-assisted synthesis was carried out in a Microwave Reaction System (Anton Paar, Netherlands) using multiple 100 mL reaction vessels. Approximately 0.020 g of silver nitrate ($AgNO_3$) was added to each of the four vessels along with 2 mL of the extract, 4 mL of deionized water and a stirrer bar. The reagent-containing vessel was reacted in the microwave at a

temperature of 90˚C for 15 minutes to a maximum temperature of 100˚C. The resultant aqueous solution of nanoparticles was collected and stored together in a dark bottle.

2.5. Synthesis of ZnONPs|GO Nanocomposite

The ZnONPs|GO nanocomposite was prepared by reducing zinc oxide directly with GO using the TAE as the reducing and stabilizing agent. Firstly, 15 mg of GO powder was dispersed in 15 mL of deionized water and ultrasonicated for 60 minutes to form a stable GO colloid followed by the addition of 20 mL of TAE while stirring. Thereafter, 1.1 mL of ammonia was added slowly to 0.54 g zinc nitrate until the resultant precipitate dissolved. The nitrate solution was then mixed with the GO and the extract-containing solution was stirred for 30 minutes. The mixture was allowed to sit undisturbed at room temperature for 2 hours followed by centrifugation resulting in a slurry-like product. The product was then washed with distilled water repeatedly to remove any impurities and finally dried overnight in an oven at 60˚C to obtain the ZnONPs|GO nanocomposite. Additionally, the conventional synthesis of ZnONPs was achieved using 40 mL of the extract in 180 mL of distilled water with 3.4 g of zinc nitrate $Zn(NO_3)_2$ solution. The mixture was stirred and heated at 80˚C for 60 minutes and on completion, it was allowed to cool at room temperature before storage. On the other hand, the microwave-assisted synthesis of ZnONPs was achieved using a mixture of 0.030 g zinc nitrate $Zn(NO_3)_2$ with 2 mL of the extract, 4 mL of deionized water and a stirrer bar in multiple 100 mL reaction vessels. The synthesis was also performed in a Microwave Reaction System at 90˚C for 15 minutes to a maximum temperature of 100˚C.

2.6. Preparation of the AgNPs|GO||GCE or ZnONPs|GO||GCE Platforms

Glassy carbon electrodes (GCE) were mechanically polished with 0.05 mm and 0.3 mm alumina slurry and then sequentially sonicated in anhydrous ethanol and distilled water for 15 min. The cleaned GCEs were dried under nitrogen followed by modification. 5.0 mg of AgNPs|GO and ZnONPs|GO nanocomposites were added separately to 2.5 mL DMF solutions and sonicated for 30 min to form stable suspensions. For each, an amount of 5.0 µL was taken and drop cast onto the GCE surfaces, rinsed and dried under infrared lamps before use. The developed electrodes will be denoted and referred to as AgNPs|GO||GCE and ZnONPs|GO||GCE.

3. Results and Discussion

3.1. Structural Properties of AgNPs|GO and ZnONPs|GO Nanocomposites

Fourier Transform Infrared Spectroscopy (FTIR)

Studies Fourier Transform Infra-Red (FTIR) spectroscopy was employed to investigate the characteristic features of the nanocomposites. **Figure 2(a)** illustrates

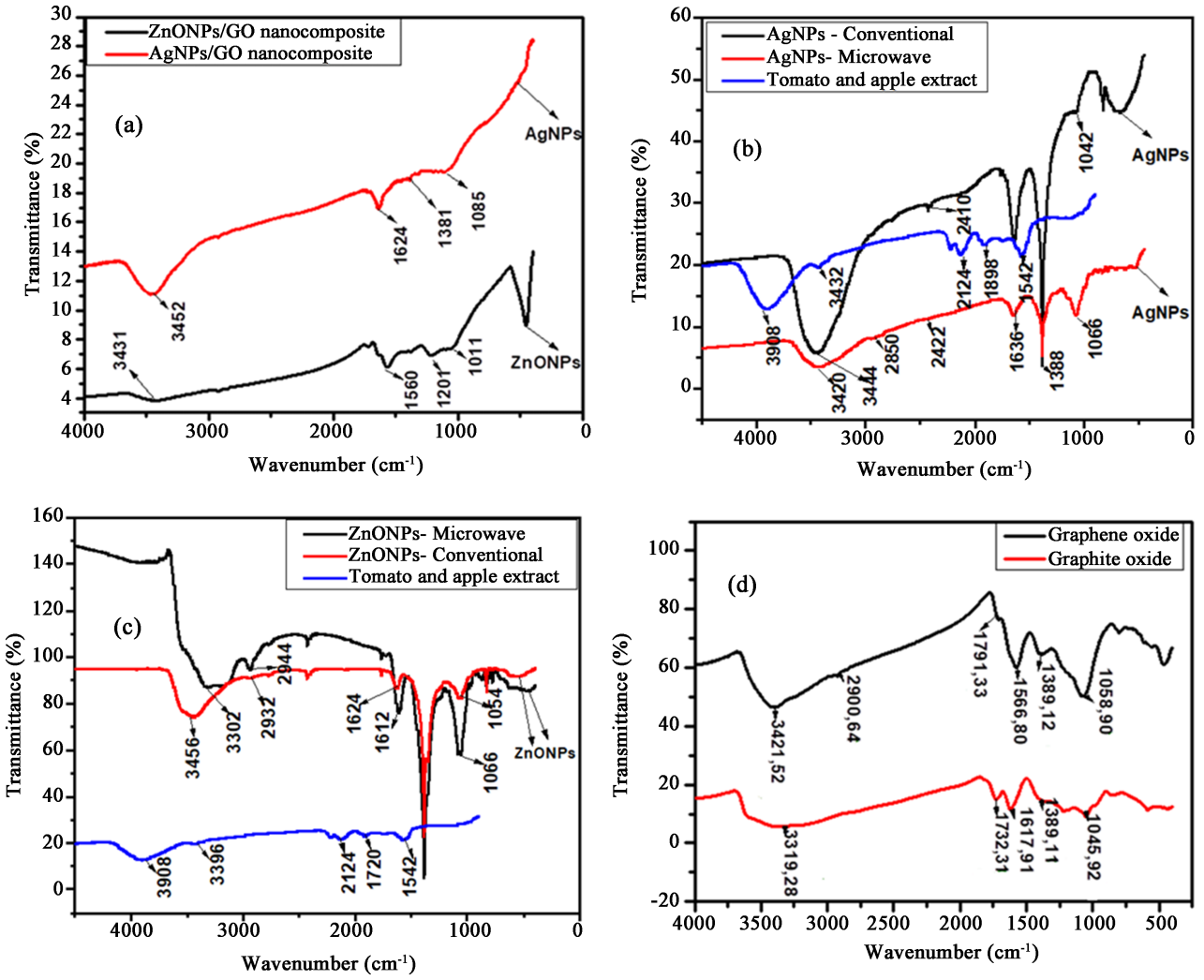

Figure 2. FTIR spectra of green synthesized (a) ZnONPs|GO and AgNPs|GO nanocomposites (b) conventionally and microwave green synthesized silver nanoparticles and TAE (c) conventional and microwave green synthesized ZnONPs and TAE and (d) graphite oxide (GrO) and graphene oxide (GO).

FTIR spectra of the green synthesized AgNPs|GO and ZnONPs|GO nanocomposites. The broad band at 3431 cm^{-1} in the FTIR spectrum of the ZnONPs|GO nanocomposite is attributed to the O–H stretching vibration of absorbed water molecules and the presence of the alcoholic substances is attributed to the TAE. The bands at 1074, 1234, and 1560 cm^{-1} are assigned to C=O stretching, sp^2 hybridized C=C groups, C–O stretching, O–H deformation and C–OH stretching respectively, confirming the presence of combined acidic and alcoholic compounds from the extracts used. Also, in the spectrum, the bands at 452 cm^{-1} correspond to the hexagonal nature of ZnO as indicated in the FTIR spectrum of ZnONPs (**Figure 2(c)**) [28]. These findings are similar to those reported in a study by Nagaraj *et al.*, 2020 [29] where graphene oxide-based zinc oxide nanocomposite was synthesized using Dalbergia latifolia leaf extracts and in which their biological applications were explored. The FTIR spectrum for AgNPs|GO nanocomposites illustrated similar bands at 1095, 1381, and 1634 cm^{-1} which are

relatively strong compared to those of ZnONPs|GO. The main band for AgNPs|GO is indicated at 3452 cm^{-1} and is attributed to the O–H stretching vibration which is attributed to the presence of the nanoparticles as seen in the conventionally synthesized nanoparticles in **Figure 2(b)**. Similar findings are reported by Gnanaprakasam *et al.*, 2014 [30] for a study using Abelmoschus esculentus extracts for the synthesis of AgNPs|GO. The band at 1560 cm^{-1} for ZnONPs|GO and at 1633 cm^{-1} for AgNPs|GO is attributed to the skeletal vibration of the graphene sheets. The additional stretching vibrations result from a combination of acidic and alcoholic compounds from apples and tomatoes. These results also evidently prove that GO (**Figure 2(d)**) was successfully exfoliated and that there is a strong interaction between AgNPs and ZnONPs with the remaining surface hydroxyl groups [31].

3.2. Ultraviolet-Visible Spectroscopy (UV-vis)

Ultraviolet Visible Spectroscopy (UV-vis) was used to study the electronic transitions of the green synthesized AgNPs|GO and ZnONPs|GO nanocomposites (**Figure 3(a)**). The UV-vis spectrum of AgNPs|GO showed typical characteristics features such as a shoulder at 213.9 nm corresponding to a π–π^* plasmon transition. The UV-visible spectrum of AgNPs|GO illustrates that there are AgNPs attached to the layers of graphene oxide by showing a typical characteristic band that is consistent with the surface plasmon resonance phenomena of AgNPs formulation as shown in **Figure 3(c)**, while GO showed a typical band around 208 nm as illustrated in (**Figure 3(b)**) corresponding to the C=C aromatic bonding [32]. These findings are consistent with those reported in a study by Alsharaeh *et al.*, 2017 [33] in which AgNPs|GO were synthesized using lemon juice extracts. The intensities and wavelengths are slightly different in this study since only one extract was used as opposed to our study. The UV–vis absorption spectrum of ZnONPs|GO revealed a characteristic absorption band at a wavelength of 205.6 nm, which was assigned to the intrinsic band gap absorption of π–π^*, owing to the electron transitions from the valence band to the conduction band. It is clearly seen that the peak position of the UV–vis spectrum of ZnONPs|GO has been affected by the absorption contribution from both ZnONPs (**Figure 3(d)**) and GO through the modification of the fundamental process of electron-hole pair formation. Although these findings are very similar to those reported by Lin *et al.*, 2020 [34]; the two extracts used in this study caused lower wavelength readings as opposed to their study where a precipitation method was used to synthesize ZnONPs|GO. This is also noteworthy due to the small nature of the nanoparticles produced in this study. Therefore, from the spectrum in **Figure 3(a)** the presence of AgNPs|GO compared to ZnONPs|GO has increased absorption and intensity which is a beneficial character for sensor performance.

3.3. Raman Spectroscopy

Raman spectroscopy is one of the most non-destructive and powerful techniques

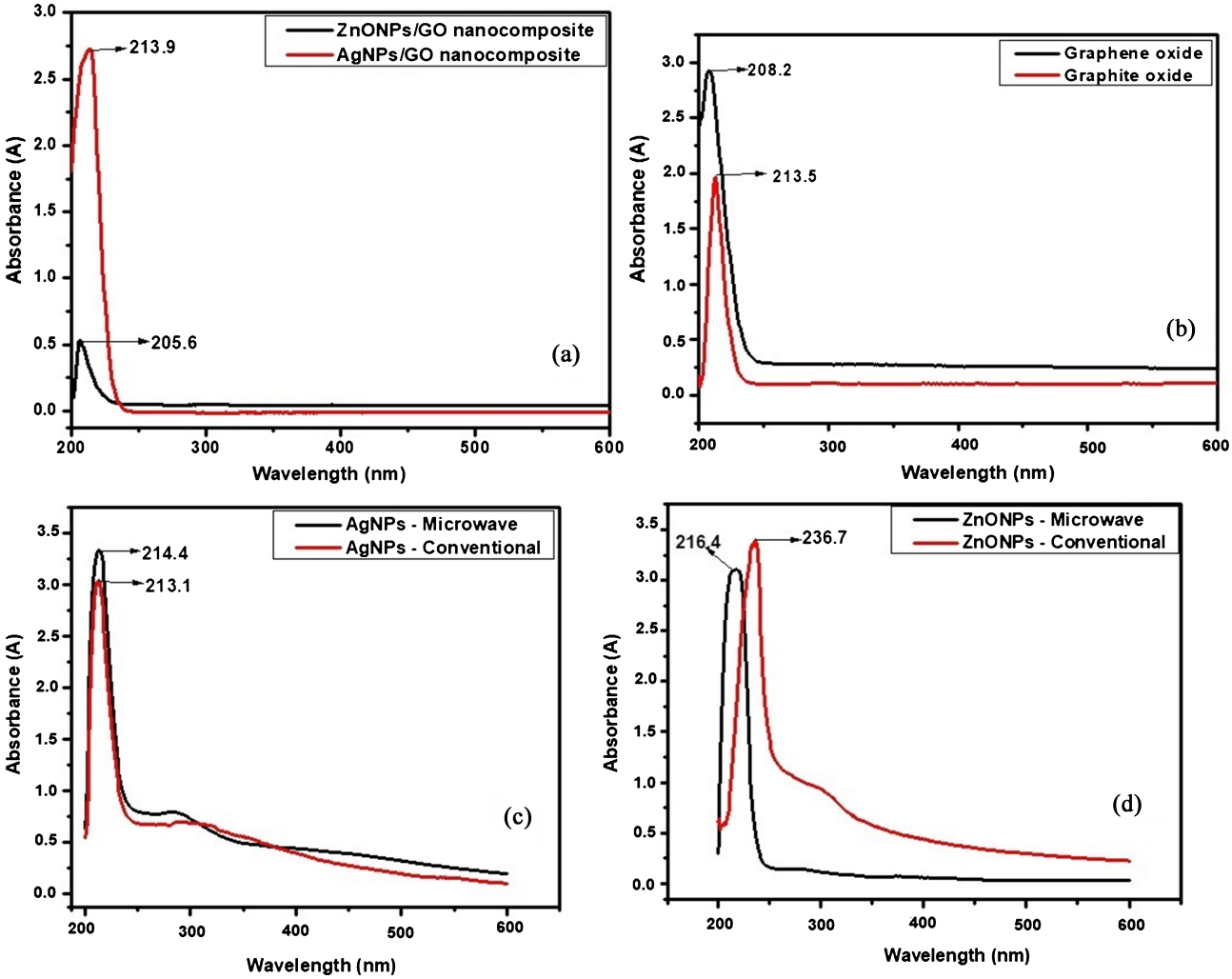

Figure 3. UV-vis spectrum of (a) green synthesized ZnONPs|GO and AgNPs|GO nanocomposites (b) graphene oxide (c) conventionally and microwave synthesized AgNPs and (d) conventionally and microwave synthesized ZnONPs.

to extract useful structural information about nanocomposites. **Figure 4** illustrates the Raman spectra obtained illustrating the D and G bands for both nanocomposites. The D band arises due to disorders at the edges of graphene, while the G band is due to in-phase vibrations of the graphene lattice. For AgNPs|GO, the D and G bands were estimated to be at approximately 1347 cm^{-1} and 1608 cm^{-1}, respectively. The G band narrates the tangential stretching mode of the E^2g phonon of the sp^2 carbon atom and the D band offers evidence of the breathing mode of the κ-point [32] [33] [34] [35]. Alternatively, for ZnONPs|GO the D and G bands were estimated to be at approximately 1339 cm^{-1} and 1577 cm^{-1}, respectively an indication that ZnONPs were anchored onto the GO surface. The intensity ratio in the Raman spectrum of ZnONPs|GO was found to be 1.17 while that of AgNPs|GO was found to be 1.19. The decreased intensity of the D peak with respect to the G peak observed indicates that there was a different restoration of the sp^2 network on the surface of graphene oxide and a reduction of nanoparticles anchored on graphene. Therefore, from the

Raman spectra, it is observed that there is the attachment of ZnONPs or AgNPs onto the GO matrix leading to partial restoration of the sp^2 network. Both these results are consistent with previous reports on the Raman spectra of AgNPs|GO and of ZnONPs|GO [34] [35] [36].

3.4. X-Ray Diffraction (XRD)

X-Ray diffraction (XRD) is a suitable technique for determining crystalline structure and interlayer distances of substances. Figure 5 illustrates XRD patterns

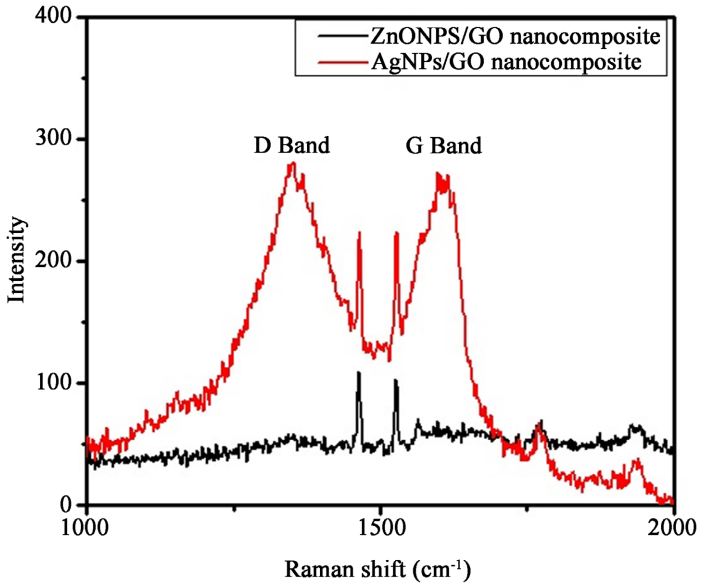

Figure 4. Raman spectra of green synthesized ZnONPs|GO and AgNPs|GO nanocomposites.

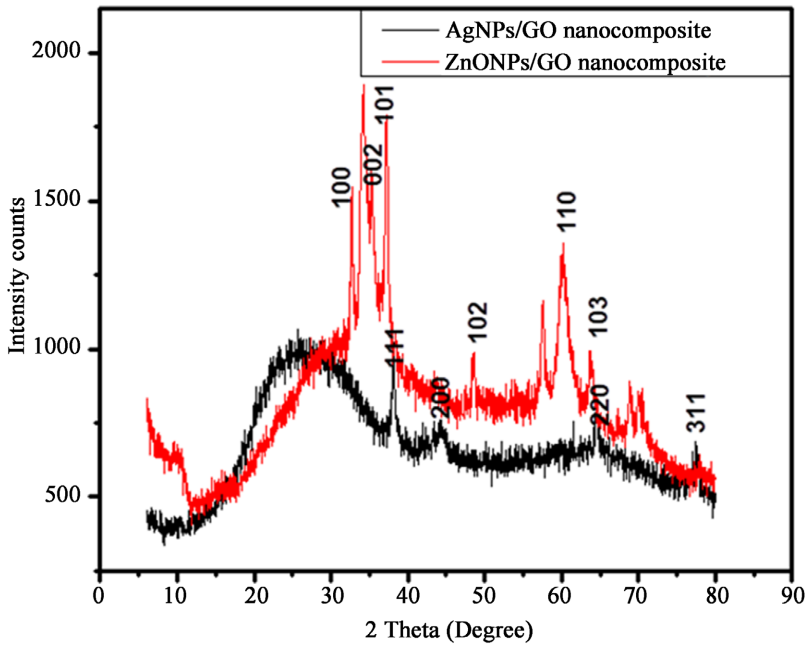

Figure 5. X-Ray diffraction spectra of green synthesized ZnONPs|GO and AgNPs|GO nanocomposites.

of both green synthesized AgNPs|GO and of ZnONPs|GO nanocomposites. For the ZnONPs|GO nanocomposite the appearance of characteristic diffraction peaks is illustrated by the red curve. The ZnO nanoparticles present in ZnONPs|GO corresponds to the (100), (002), (101), (102), (110), (103), and (112) crystal lattice planes. All these diffraction peaks confirm that crystalline ZnO has a hexagonal quartzite structure while the sharp diffraction peak at $2\theta =$ 10.16˚ is a confirmation of the presence of GO [37]. Moreover, the disappearance of the (001) reflection of GO in the XRD pattern of ZnONPs|GO is attributed to the intercalation of ZnONPs that impaired the regular stack of graphene oxide [38]. The XRD pattern for the AgNPs|GO nanocomposite illustrated amorphous phases with peaks at approximately 38.2˚, 44.2˚, 64.6˚ and 77.5˚ which were allocated to the (111), (200), (220) and (311) crystal lattice planes of face-cantered cubic (fcc) silver nanoparticles while the peak for GO disappeared due to the attachment of the nanoparticles onto the inlayers of GO which led to shielding the signals of the GO peaks. Evidently, the sharp peak at 38.2˚ confirmed that the nanoparticles are composed of pure crystalline silver [39].

3.5. Microscopic Properties of AgNPs|GO and ZnONPs|GO Nanocomposites

The representative HRTEM images of AgNPs|GO and ZnONPs|GO nanocomposite is shown in **Figure 6(a)** and **Figure 6(b)**, respectively. In both images, large GO sheets with dimensions in the nanometers range were found positioned at the top of the grid where rippled silk waves and transparent appearances where demonstrated. In the case of the HRTEM image of ZnONPs|GO (**Figure 6(b)**), the dark spots on the GO flake are attributed to the presence of ZnONPs and were determined to be between 3 and 9 nm. As a result, the image proves that the nanoparticles and nanosheet GO are present in the nanocomposite. Similar findings are reported in a study by Ezeigwe *et al.*, 2014 [40] where

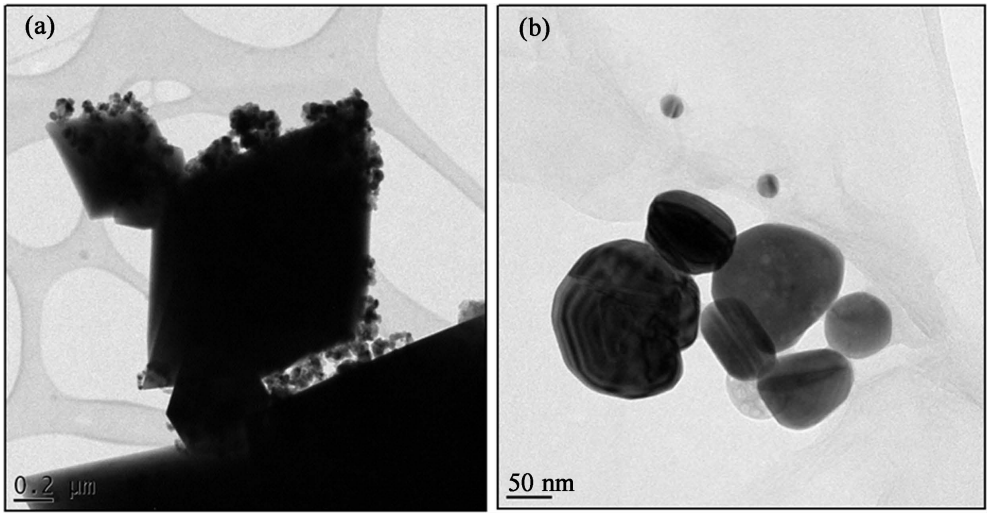

Figure 6. HRTEM images of green synthesized (a) ZnONPs|GO and (b) AgNPs|GO nanocomposites.

ZnONPs|GO was synthesized in a one-step process for application in electrochemical capacitors. For the AgNPs|GO nanocomposite (**Figure 6(a)**) the GO sheets are observed with few crumpled silk waves while the oval or spherical shape AgNPs are evident on the GO sheets. The examined particle sizes were determined to be between 8 and 12 nm. Zeng *et al.*, 2016 [41] also reported similar HRTEM images and particle sizes in a study using four different green reducing agents for the synthesis of AgNPs|GO nanocomposites.

HRSEM was used to further study the surface morphology of AgNPs|GO and ZnONPs|GO nanocomposites as shown in **Figure 7(a)** and **Figure 7(b)**. The HRSEM images of ZnONPs|GO (**Figure 7(a)**) illustrate ZnONPs and uniformly dispersed covered on rippled GO silk wave sheets while some ZnONPs are seen to be agglomerated. In the case of AgNPs|GO (**Figure 7(b)**), the AgNPs were

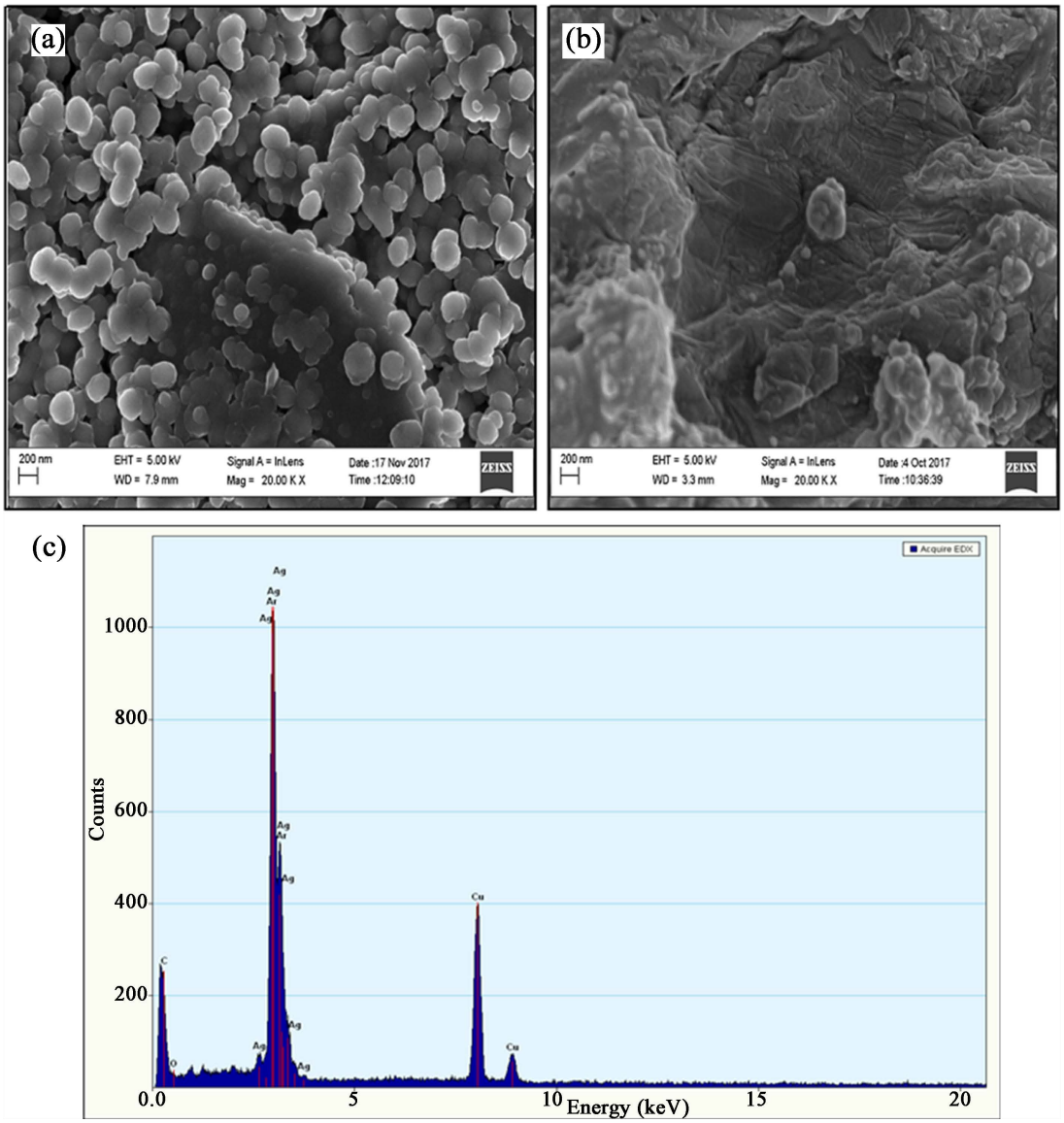

Figure 7. HRSEM images of green synthesized (a) ZnONPs|GO, (b) AgNPs|GO nanocomposites and (c) the EDX spectrum of AgNPs|GO nanocomposites.

randomly and well distributed onto grumbled GO silk wave sheets. The AgNPs|GO images are consistent with a study by Vi *et al.*, 2018 [42] involving the synthesis and characterization of graphene oxide-silver nanocomposite even thorough a conventional method was utilized.

Due to the unclear nature of Figure 7(b), the sample was also studied using Energy-dispersive X-rays spectroscopy (EDX) (Figure 7(c)) in order to determine the elemental composition (Table 1) of the green synthesized AgNPs/GO nanocomposites in order to prove the attachment of the AgNPs on GO.

The EDX spectrum for AgNPs/GO clearly illustrated the Ag peak indicating the presence of silver nanoparticles therein the sample. The elements that were present and listed as percentage values were, oxygen (O) peak was from graphene oxide present in the nanocomposite and the presence of copper (Cu) results from copper grids used throughout for sample preparation to precede the analyses.

3.6. Electrochemical Characterisation of TAE|AgNPs|GO and TAE|ZnONPs|GO Nanocomposites

Cyclic Voltammetry (CV)

The electrochemical responses of green synthesized AgNPs|GO nanocomposites and ZnONPs|GO nanocomposites are illustrated in Figure 8. Represented here

Table 1. Elemental composition of AgNPs/GO nanocomposite.

Element	Weight Percentage (%)	Weight Percentage Sigma (%)
C	19.02	2.77
O	23.07	3.66
Ag	57.9	3.66
Total:	**100**	

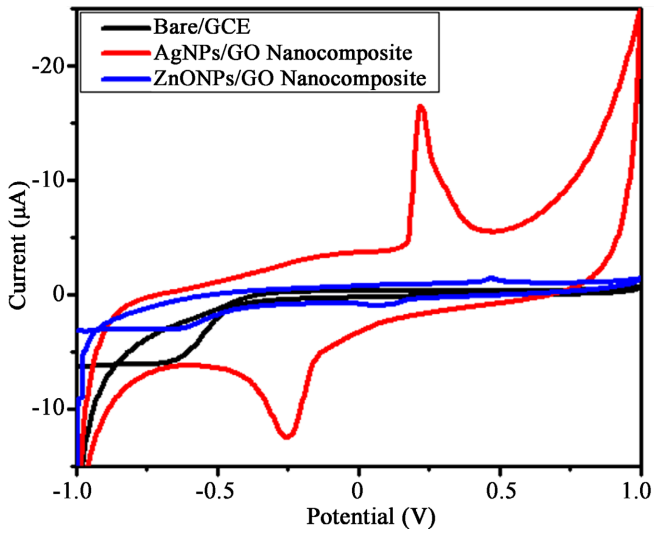

Figure 8. CV of bare glassy carbon electrode (GCE) (black curve), green synthesized AgNPs|GO nanocomposite (red curve) and green synthesized ZnONPs|GO nanocomposite (blue curve) in phosphate buffer solution (pH 7.4) at 30 mV s^{-1}.

is a bare glassy carbon (GC) electrode (black curve), AgNPs|GO||GC electrode (red curve) and ZnONPs|GO||GC electrode (blue curve) evaluated in 0.1 M PBS, pH7.4 buffer at a scan rate of 30 mV/s and at a potential window of −1000 to 1000 mV. The potential window demonstrates a well-defined redox couple of anodic and cathodic peaks for both nanocomposites. The results shown indicate that ZnONPs|GO||GC and AgNPs|GO||GC have different redox responses compared to the bare GCE. The anodic and cathodic current peaks of the nanocomposites increased linearly with increased scan rates with slight positive shifts in the potential values. The shift is indicative of the electrochemical nature of the nanocomposites [43].

Moreover, the effect of scan rate on the peak current was examined by running a series of cyclic voltammograms at different scan rates from 10 to 100 mV s^{-1} as shown in **Figure 9(a)** and **Figure 9(b)** where the ZnONPs|GO||GC and AgNPs|GO||GC electrodes were studied independently. The results presented by CV display that the anodic peak current varies linearly with the scan rate and a shift in the potential to more positive values with increasing scan rate was observed for each attached nanocomposite. This indicates that these nanocomposites were conductive while transferring electrons with the electrode surface. CV analysis of these nanocomposites at different scan rates led to the preparation of linear plots (not shown) whose slopes provide additional information about the redox properties of the nanocomposites. The slopes of plots of log scan rate versus log current were used to identify adsorption-controlled or diffusion-controlled processes. The plot for the green synthesized ZnONPs|GO||GC electrode revealed the linear equation y = 0.6071x − 0.7595 with correlation coefficient (r^2) of 0.9955 while that for AgNPs|GO||GC revealed the linear equation of y = 0.7341x + 0.0873 and correlation coefficient (r^2) of 0.9865. The slopes of these equations indicate that the electron transfer reactions for each nanocomposite were adsorption controlled. Additionally, the analysis of the peak-to-peak separations (ΔE_p) for each nanocomposite was determined and confirmed that the electrochemical processes were classified as quasi-reversible since ΔE_p was determined to be larger than the value of 57/n mV associated with the reversible process at 25˚C within the scan rates employed [44].

Furthermore, the Brown-Anson equation (Equation (1)) was used to determine the surface concentration Γ* (mol·cm^{-2}) of the nanocomposites. From the equation, F is the faraday constant (96485 C·mol^{-1}), A is the surface area of the glassy carbon electrode (3.00 mm), n is the number of electrons transferred, υ is the scan rate (V·s^{-1}), T is the operating absolute temperature of the system (25˚C T in 298 K), R is the gas constant (8.314 J·mol^{-1}·K^{-1}), Γ* represent the surface concentration of the AgNPs|GO and ZnONPs|GO (mol·cm^{-2}). The surface concentration (Γ*) of AgNPs|GO nanocomposite was established to be 7.1854×10^{-4} mol·cm^{-2} while that of ZnONPs|GO nanocomposite was determined to be 5.8645×10^{-3} mol·cm^{-2}. This indicates that the AgNPs|GO nanocomposite is less dense than that of ZnONPs|GC nanocomposite as indicated by the reduced surface

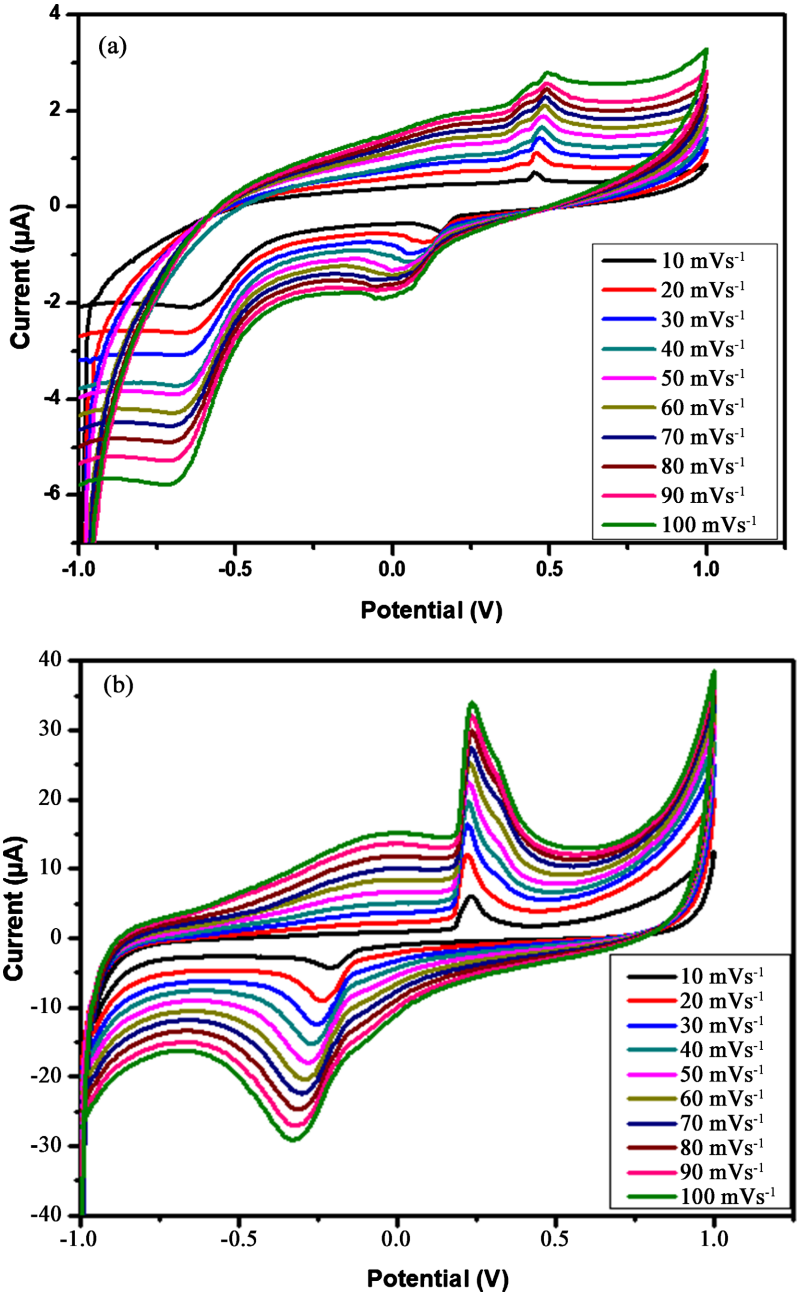

Figure 9. CV of green synthesized (a) ZnONPs|GO nanocomposite (b) AgNPs|GO nanocomposite in 0.1 M phosphate buffer solution (pH 7.4) at 10-100 mV·s^{-1}.

concentration value.

$$\frac{I_p = n^2F^2\Gamma^* A\nu}{4RT} \quad (1)$$

Similarly, the diffusion coefficient of the nanocomposites was determined using the Randel-Sevcik Equation (Equation (2)). For the AgNPs|GO nanocomposite a value of 1.8213×10^{-4} cm^2/s was determined and a value of 1.5979×10^{-4} cm^2/s was determined for the ZnONPs|GC nanocomposite. As predicted the value observed for the AgNPs|GO nanocomposite is slightly higher than that observed for

the ZnONPs|GO nanocomposite an indication of a faster electron transfer reaction taking place. Thus, the AgNPs|GO nanocomposite allows efficient transfer of electrons hence it would be preferred towards sensor development [45] [46] [47].

$$I_p = 0.4463nFAC\left(\frac{nF\nu D_e}{RT}\right)^{1/2} \quad (2)$$

A study by Low *et al.*, 2016 [48] is an illustration of the use of ZnONPs|GO nanocomposites in sensor construction. Similarly, a facile and green approach has been used in this study to synthesize highly electroactive sensor platforms which have been used successfully for the detection of single-stranded RNA. Furthermore, Ajayi *et al.*, 2020 [49] also reported on the use of pear-capped AgNPs|GO nanocomposites in the construction of electrochemical sensors for the detection of Tuberculosis treatment drugs. This is enough evidence to illustrate the potential use of the reported AgNPs|GO and ZnONPs|GO in sensor applications.

4. Conclusion

This study reports for the first time the use of apple (*Malus domestica*) and tomato (*Solanum lycopersicum*) extracts for the green method synthesis of AgNPs|GO and ZnONPs|GO nanocomposite by means of conventional heating. The structural properties of the nanocomposites were interrogated by means of Fourier Transform Infra-Red spectroscopy and Raman spectroscopy where the role of the apple and tomato extracts was evident in the synthesis of the nanocomposites as demonstrated by the recorded functional groups. Optical studies with Ultraviolet-visible spectroscopy revealed the absorbance bands attributed to the nanoparticles embedded in the graphene oxide sheet while the morphology of the nanocomposites was determined using High-Resolution Scanning Electron Microscopy and High-Resolution Transmission Electron Microscopy in which the size of the embedded nanoparticles was determined to be 8 to 12 nm for AgNOs and 3 to 9 nm for ZnONPs. The nanocomposite was later compared since they showed a good degree of dispersion as well as excellent size distribution which contributed to the good electrochemical properties of these nanocomposites as observed through voltammetric studies. The AgNPs|GO nanocomposites were established to have a higher diffusion coefficient than the ZnONPs|GO nanocomposites an indication of their superior ability to be used in sensor development.

Acknowledgements

We thank the staff at iThembaLabs, SensorLab, the Chemistry and Physics Departments at the University of the Western Cape for the analysis of samples generated from this study. The National Research Foundation, South Africa is appreciated for funding the project and the Council for Scientific and Industrial Research, South Africa is also appreciated for funding the students involved in this study.

Conflicts of Interest

The authors declare no conflicts of interest regarding the publication of this paper.

References

[1] Shafiq, M., Anjum, S., Hano, C., Anjum, I. and Haider Abbasi, B. (2020) An Overview of the Applications of Nanomaterials and Nanodevices in the Food Industry. *Foods*, **9**, Article 148. https://doi.org/10.3390/foods9020148

[2] Taheriniya, S. and Behboodi, Z. (2016) Comparing Green Chemical Methods and Chemical Methods for the Synthesis of Titanium Dioxide Nanoparticles. *International Journal of Pharmaceutical Sciences and Research*, **7**, 4927-4932.

[3] Makarov, V.V., Love, A.J., Sinitsyna, O.V., Makarova, S.S., Yaminsky, I.V., Taliansky, M.E. and Kalinina, N.O. (2014) "Green" Nanotechnologies: Synthesis of Metal Nanoparticles Using Plants. *Acta Naturae*, **6**, 35-44. https://doi.org/10.32607/20758251-2014-6-1-35-44

[4] Quyen, T.T.B., Minh, T.A., Thuy, N.T.P. and Mai, T.T.X. (2017) A Green Approach Using River-Leaf Creeper Extract for Synthesis and Characterization of Chitosan/Ag Nanocomposites and Study for Their Antibacterial Activity. *International Journal of Engineering Science Invention*, **6**, 76-81.

[5] Zaaba, N.I., Foo, K.L., Hashim, U., Tan, S.J., Liu, W.W. and Voon, C.H. (2017) Synthesis of Graphene Oxide Using Modified Hummers Method: Solvent Influence. *Procedia Engineering*, **184**, 469-477. https://doi.org/10.1016/j.proeng.2017.04.118

[6] Li, F., Jiang, X., Zhao, J. and Zhang, S. (2015) Graphene Oxide: A Promising Nanomaterial for Energy and Environmental Applications. *Nano Energy*, **16**, 488-515. https://doi.org/10.1016/j.nanoen.2015.07.014

[7] Paulchamy, B., Arthi, G. and Lignesh, B.D. (2015) A Simple Approach to Stepwise Synthesis of Graphene Oxide Nanomaterial. *Journal of Nanomedicine & Nanotechnology*, **6**, Article ID: 1000253. https://doi.org/10.4172/2157-7439.1000253

[8] Narayanan, K.B. and Sakthivel, N. (2011) Green Synthesis of Biogenic Metal Nanoparticles by Terrestrial and Aquatic Phototrophic and Heterotrophic Eukaryotes and Biocompatible Agents. *Advances in Colloid and Interface Science*, **169**, 59-79. https://doi.org/10.1016/j.cis.2011.08.004

[9] Nasrollahzadeh, M., Sajjadi, M., Sajadi, S.M. and Issaabadi, Z. (2019) Green Nanotechnology. In: Hubbard, A., Ed., *Interface Science and Technology*, Elsevier B.V., Amsterdam, 145-198. https://doi.org/10.1016/B978-0-12-813586-0.00005-5

[10] Alamdari, S., Ghamsari, M.S., Lee, C., Han, W., Park, H., Tafreshi, M.J., Afarideh, H. and Ara, M.H.M (2020) Preparation and Characterization of Zinc Oxide Nanoparticles Using Leaf Extract of Sambucus Ebulus. *Applied Sciences*, **10**, Article 3620. https://doi.org/10.3390/app10103620

[11] Srikar, S.K., Giri, D.D., Upadhyay, C., Mishra, P.K. and Upadhyay, S.N. (2015) Green Synthesis of Silver Nanoparticles Using Prunus Amygdalus Extract and Their Anti-Microbial Activity. *Advanced Materials Research*, **1119**, 165-169. https://doi.org/10.4028/www.scientific.net/AMR.1119.165

[12] Nguyen, V.H., Papanastasiou, D.T., Resende, J., Bardet, L., Sannicolo, T., Jiménez, C., Muñoz-Rojas, D., Nguyen, N.D. and Bellet, D. (2022) Advances in Flexible Metallic Transparent Electrodes. *Small*, **18**, Article ID: 2106006. https://doi.org/10.1002/smll.202106006

[13] Zhao, H., Yang, J., Wang, L., Tian, C., Jiang, B. and Fu, H. (2011) Fabrication of a Palladium Nanoparticle/Graphene Nanosheet Hybrid *via* Sacrifice of a Copper Template and Its Application in Catalytic Oxidation of Formic Acid. *Chemical Communications*, **47**, 2014-2016. https://doi.org/10.1039/c0cc04432f

[14] Upadhyay, R.K., Soin, N., Bhattacharya, G., Saha, S., Barman, A. and Roy, S.S. (2015) Grape Extract Assisted Green Synthesis of Reduced Graphene Oxide for Water Treatment Application. *Materials Letters*, **160**, 355-358. https://doi.org/10.1016/j.matlet.2015.07.144

[15] Li, J., Liu, J., Tan, G., Jiang, J., Peng, S., Deng, M., Qian, D., Feng, Y. and Liu, Y. (2014) High-Sensitivity Paracetamol Sensor Based on Pd/Graphene Oxide Nanocomposite as an Enhanced Electrochemical Sensing Platform. *Biosensors and Bioelectronics*, **54**, 468-475. https://doi.org/10.1016/j.bios.2013.11.001

[16] Li, J., Kuang, D., Feng, Y., Zhang, F., Xu, Z., Liu, M. and Wang, D. (2013) Green Synthesis of Silver Nanoparticles-Graphene Oxide Nanocomposite and Its Application in Electrochemical Sensing of Tryptophan. *Biosensors and Bioelectronics*, **42**, 198-206. https://doi.org/10.1016/j.bios.2012.10.029

[17] Low, S.S., Tan, M.T.T., Khiew, P.S., Loh, H. and Chiu, W.S. (2015) One Step Green Synthesis of Graphene/ZnO Nanocomposite for Nonenzymatic Hydrogen Peroxide Sensing. *Materials and Technology*, **49**, 837-840. https://doi.org/10.17222/mit.2014.259

[18] Pattanayak, M. and Nayak, P.L. (2014) Green Synthesis of Gold Nanoparticles Using Solanus Lycopersicum (TOMATO) Aqueous Extract. *World Journal of Nano Science & Technology*, **3**, 74-80.

[19] Santiago, T.R., Bonatto, C.C., Rossato, M., Lopes, C.A.P., Lopes, C.A. Mizubuti, E.S.G. and Silva, L.P. (2019) Green Synthesis of Silver Nanoparticles Using Tomato Leaf Extract and Their Entrapment in Chitosan Nanoparticles to Control Bacterial Wilt. *Journal of Science Food and Agriculture*, **9**, 4248-4259. https://doi.org/10.1002/jsfa.9656

[20] Wilkerson, D.E., Anthon, G.E., Barrett, D., Sayajon, G., Santos, A.M. and Rodriguez-Saona, L.E. (2013) Rapid Assessment of Quality Parameters in Processing Tomatoes Using Hand-Held and Benchtop Infrared Spectrometers and Multivariate Analysis. *Journal of Agricultural and Food Chemistry*, **61**, 2088-2095. https://doi.org/10.1021/jf304968f

[21] Sutradhar, P. and Saha, M. (2016) Green Synthesis of Zinc Oxide Nanoparticles Using Tomato (*Lycopersicon esculentum*) Extract and Its Photovoltaic Application. *Journal of Experimental Nanoscience*, **11**, 314-327. https://doi.org/10.1080/17458080.2015.1059504

[22] Mirzaa, A.U., Kareema, A., Namib, S.A.A., Bhata, S.A., Mohammada, A. and Nishata, N. (2019) *Malus pumila* and *Juglen regia* Plant Species Mediated Zinc Oxide Nanoparticles: Synthesis, Spectral Characterization, Antioxidant and Antibacterial Studies. *Microbial Pathogenesis*, **129**, 233-241. https://doi.org/10.1016/j.micpath.2019.02.020

[23] Umoren, S.A, Obot, I.B. and Gasem, Z.M. (2014) Green Synthesis and Characterization of Silver Nanoparticles Using Red Apple (*Malus domestica*) Fruit Extract at Room Temperature. *Journal of Materials and Environmental Science*, **5**, 907-914.

[24] Ali, Z.A., Yahya, R., Sekaran, S.D. and Puteh, R. (2016) Green Synthesis of Silver Nanoparticles Using Apple Extract and Its Antibacterial Properties. *Advances in Materials Science and Engineering*, **2016**, Article ID: 4102196. https://doi.org/10.1155/2016/4102196

[25] Kazlagić, A., Abud, O.A., Ćibo, M., Hamidović, S., Borovac, B. and Omanović-Mikličanin, E. (2020) Green Synthesis of Silver Nanoparticles Using Apple Extract and Its Antimicrobial Properties. *Health and Technology*, **10**, 147-150. https://doi.org/10.1007/s12553-019-00378-5

[26] Alves, M.M., Andrade, S.M., Grenho, L., Fernandes, M.H., Santos, C. and Montemora, M.F. (2019) Influence of Apple Phytochemicals in ZnO Nanoparticles Formation, Photoluminescence and Biocompatibility for Biomedical Applications. *Materials Science and Engineering*: *C*, **101**, 76-87. https://doi.org/10.1016/j.msec.2019.03.084

[27] Alam, S.N., Sharma, N. and Kumar, L. (2017) Synthesis of Graphene Oxide (GO) by Modified Hummers Method and Its Thermal Reduction to Obtain Reduced Graphene Oxide (rGO). *Graphene*, **6**, 1-18. https://doi.org/10.4236/graphene.2017.61001

[28] Azarang, M., Shuhaimi, A. Yousefi, R. Golsheikh, A.M. and Sookhakian, M. (2014) Synthesis and Characterization of ZnO NPs/Reduced Graphene Oxide Nanocomposite Prepared in Gelatin Medium as Highly Efficient Photo-Degradation of MB. *Ceramics International*, **40**, 10217-10221. https://doi.org/10.1016/j.ceramint.2014.02.109

[29] Nagaraj, E., Shanmugam, P., Karuppannan, K., Chinnasamyb, T. and Venugopal, S. (2020) The Biosynthesis of a Graphene Oxide-Based Zinc Oxide Nanocomposite Using Dalbergia Latifolia Leaf Extract and Its Biological Applications. *New Journal of Chemistry*, **44**, 2166-2179. https://doi.org/10.1039/C9NJ04961D

[30] Gnanaprakasama, P. and Selvaraju, T. (2014) Green Synthesis of Self Assembled Silver Nanowire Decorated Reduced Graphene Oxide for Efficient Nitroarene Reduction. *RSC Advances*, **4**, 24518-24525. https://doi.org/10.1039/C4RA01798F

[31] Shao, W., Liu, X., Min, H., Dong, G., Feng, Q. and Zuo, S. (2015) Preparation, Characterization, and Antibacterial Activity of Silver Nanoparticle-Decorated Graphene Oxide Nanocomposite. *ACS Applied Materials & Interfaces*, **7**, 6966-6973. https://doi.org/10.1021/acsami.5b00937

[32] Gurunathan, S. and Kim, J.H. (2017) Graphene Oxide-Silver Nanoparticles Nanocomposite Stimulates Differentiation in Human Neuroblastoma Cancer Cells (SH-SY5Y). *International Journal of Molecular Sciences*, **18**, Article 2549. https://doi.org/10.3390/ijms18122549

[33] Alsharaeh, E., Alazzam, S., Ahmed, F., Arshi, N., Al-Hindawi, M. and Sing, G.K. (2017) Green Synthesis of Silver Nanoparticles and Their Reduced Graphene Oxide Nanocomposites as Antibacterial Agents: A Bio-Inspired Approach. *Acta Metallurgica Sinica* (*English Letters*), **30**, 45-52. https://doi.org/10.1007/s40195-016-0485-z

[34] Lin, Y., Hong, R., Chen, H., Zhang, D. and Xu, J. (2020) Green Synthesis of ZnO-GO Composites for the Photocatalytic Degradation of Methylene Blue. *Journal of Nanomaterials*, **2020**, Article ID: 4147357. https://doi.org/10.1155/2020/4147357

[35] Rajesh, A., Mangamma, G., Sairam, T.N., Subramanian, S., Kalavathi, S., Kamruddin, M. and Dash, S. (2017) Physicochemical Properties of Nanocomposite: Hydroxyapatite in Reduced Graphene Oxide. *Materials Science and Engineering*: *C*, **76**, 203-210. https://doi.org/10.1016/j.msec.2017.02.044

[36] Jilani, S.M. and Banerji, P. (2014) Graphene Oxide-Zinc Oxide Nanocomposite as Channel Layer for Field Effect Transistors: Effect of ZnO Loading on Field Effect Transport. *ACS Applied Materials & Interfaces*, **6**, 16941-16948.

https://doi.org/10.1021/am504501n

[37] Zhong, L. and Yun, K. (2015) Graphene Oxide-Modified ZnO Particles: Synthesis, Characterization, and Antibacterial Properties. *International Journal of Nanomedicine*, **10**, 79-92. https://doi.org/10.2147/IJN.S88319

[38] Hosseini, S.A. and Babaei, S. (2017) Graphene Oxide/Zinc Oxide (GO/ZnO) Nanocomposite as a Superior Photocatalyst for Degradation of Methylene Blue (MB)-Process Modeling by Response Surface Methodology (RSM). *Journal of the Brazilian Chemical Society*, **28**, 299-307. https://doi.org/10.5935/0103-5053.20160176

[39] Roy, I., Rana, D., Sarkar, G., Bhattacharyya, A., Saha, N.R., Mondal, S., Pattanayak, S., Chattopadhyay, S. and Chattopadhyay, D. (2015) Physical and Electrochemical Characterization of Reduced Graphene Oxide/Silver Nanocomposites Synthesized by Adopting a Green Approach. *RSC Advances*, **5**, 25357-25364. https://doi.org/10.1039/C4RA16197A

[40] Ezeigwe, E.R., Tan, M.T.T., Kheiw, P.S. and Khiewa, C.W. (2015) Siong, One-Step Green Synthesis of Graphene/ZnO Nanocomposites for Electrochemical Capacitors. *Ceramics International*, **41**, 715-724. https://doi.org/10.1016/j.ceramint.2014.08.128

[41] Zeng, J., Tian, X., Song, J., Wei, Z., Harrington, S., Yao, Y., Ma, L. and Ma, Y. (2016) Green Synthesis of AgNPs/Reduced Graphene Oxide Nanocomposites and Effect on the Electrical Performance of Electrically Conductive Adhesives. *Journal of Material Science*: *Materials in Electronics*, **27**, 3540-3548. https://doi.org/10.1007/s10854-015-4189-3

[42] Vi, T.T.T., Kumar, S.R., Rout, B., Liu, C., Wong, C., Chang, C., Chen, C.D., Chen, W. and Lue, S.J. (2018) The Preparation of Graphene Oxide-Silver Nanocomposites: The Effect of Silver Loads on Gram-Positive and Gram-Negative Antibacterial Activities. *Nanomaterials*, **8**, Article 163. https://doi.org/10.3390/nano8030163

[43] Arfin, T. and Rangari, S.N. (2018) Graphene Oxide-ZnO Nanocomposite Modified Electrode for the Detection of Phenol. *Analytical Methods*, **10**, 347-358. https://doi.org/10.1039/C7AY02650A

[44] Sakthivel, R., Annalakshmi, M., Chen, S.M. and Kubendhiran, S. (2019) Efficient Electrochemical Detection of Lethal Environmental Pollutant Hydroquinone Based on Functionalized Carbon Black/Polytyramine/Gold Nanoparticles Nanocomposite. *Journal of the Electrochemical Society*, **166**, B680. https://doi.org/10.1149/2.0671908jes

[45] Rajabathar, J.R., Shukla, A.K., Ali, A. and Al-Lohedan, H.A. (2017) Silver Nanoparticle/R-Graphene Oxide Deposited Mesoporous-Manganese Oxide Nano-composite for Pollutant Removal and Supercapacitor Applications. *International Journal of Hydrogen Energy*, **42**, 15679-15688. https://doi.org/10.1016/j.ijhydene.2017.04.038

[46] Feleni, U., Ajayi, R. F., Jijana, A., Sidwaba, U., Douman, S., Baker, P.G.L. and Iwuoha, E. (2016) Tin Selenide Quantum Dots Electrochemical Biotransducer for the Determination of Indinavir—A Protease Inhibitor Anti-Retroviral Drug. *Journal of Nano Research*, **44**, 196-207. https://doi.org/10.4028/www.scientific.net/JNanoR.44.196

[47] Devi, R., Gogoi, S., Dutta, H.S., Bordoloi, M., Sanghi, S.K. and Khan, R. (2020) Au/$NiFe_2O_4$ Nanoparticle-Decorated Graphene Oxide Nanosheets for Electrochemical Immunosensing of Amyloid Beta Peptide. *Nanoscale Advances*, **2**, 239-248. https://doi.org/10.1039/C9NA00578A

[48] Low, H.S., Loh, J.S., Boey, P.S., Khiew, W.S., Chiu, M. and Tan, M.T.T. (2016) Sensitivity Enhancement of Graphene/Zinc Oxide Nanocomposite-Based Electro-

chemical Impedance Genosensor for Single Stranded RNA Detection. *Biosensors and Bioelectronics*, **94**, 365-373.
https://doi.org/10.1016/j.bios.2017.02.038

[49] Ajayi, R.F., Tshoko, S., Mgwili, Y., Nqunqa, S., Mulaudzi, T., Mayedwa, N. and Iwuoha, E. (2020) Green Method Synthesised Graphene-Silver Electrochemical Nanobiosensors for Ethambutol and Pyrazinamide. *Processes*, **8**, Article 879.
https://doi.org/10.3390/pr8070879